HAL
open science

Development and Experimental Demonstration of Negative First-Order Quasi-Phase Matching in a periodically-poled Rb-doped KTiOPO4 crystal

Yannick Petit, Alexandra Pena, Patricia Segonds, Jérôme Debray, Simon Joly, Andrius Zukauskas, Fredrik Laurell, Valdas Pasiskevicius, Carlota Canalias, Benoit Boulanger

To cite this version:

Yannick Petit, Alexandra Pena, Patricia Segonds, Jérôme Debray, Simon Joly, et al.. Development and Experimental Demonstration of Negative First-Order Quasi-Phase Matching in a periodically-poled Rb-doped KTiOPO4 crystal. Optics Letters, 2020, 45 (21), pp.6026-6029. 10.1364/OL.408839 . hal-02953325

HAL Id: hal-02953325

https://hal.science/hal-02953325v1

Submitted on 2 Nov 2020

HAL is a multi-disciplinary open access archive for the deposit and dissemination of scientific research documents, whether they are published or not. The documents may come from teaching and research institutions in France or abroad, or from public or private research centers.

L'archive ouverte pluridisciplinaire **HAL**, est destinée au dépôt et à la diffusion de documents scientifiques de niveau recherche, publiés ou non, émanant des établissements d'enseignement et de recherche français ou étrangers, des laboratoires publics ou privés.

Development and Experimental Demonstration of Negative First-Order Quasi-Phase Matching in a *periodically-poled Rb-doped $KTiOPO_4$* crystal

Yannick Petit,[1,2,*] Alexandra Peña,[3] Patricia Segonds,[3] Jérôme Debray,[3] Simon Joly,[4] Andrius Zukauskas,[5] Fredrik Laurell,[5] Valdas Pasiskevicius,[5] Carlota Canalias,[5] and Benoît Boulanger[3,*]

[1]Université de Bordeaux, CNRS, CEA, CELIA, UMR 5107, F-33405 Talence, France
[2]Université de Bordeaux, CNRS, ICMCB, UPR 9048, F-33608 Pessac, France
[3]Université Grenoble Alpes, CNRS, Grenoble INP, Institut Néel, 38000 Grenoble, France
[4]IMS Laboratory, University of Bordeaux, UMR CNRS 5218, 351 Cours de la Libération, 33405 Talence, France
[5]Laser Physics, Applied Physics Department, Royal Institute of Technology, AlbaNova University Center, Roslagstullsbacken 21, 10691 Stockholm, Sweden
*Corresponding authors: yannick.petit@u-bordeaux.fr, benoit.boulanger@neel.cnrs.fr

Received XX Month XXXX; revised XX Month, XXXX; accepted XX Month XXXX; posted XX Month XXXX (Doc. ID XXXXX); published XX Month XXXX

We worked on a new scheme of Quasi-Phase-Matching (QPM) based on the negative first-order of the spatial modulation of the sign of the second-order nonlinearity. Applying this scheme in the case of Angular-Quasi-Phase-Matching (AQPM) in a biaxial crystal reveals new directions of propagation for efficient parametric frequency conversion as well as "giant" spectral acceptances. The experimental validation is performed in a periodically-poled Rubidium-doped $KTiOPO_4$ biaxial crystal. This new approach naturally extends to other periodically-poled uniaxial crystals such as periodically-poled $LiNbO_3$.

© 2020 Optical Society of America

http://dx.doi.org/10.1364/OL.99.099999

Phase-matching is the privileged way to optimize the performance of nonlinear optical frequency conversion. Usually, it can be obtained by using the birefringence of anisotropic crystals, which corresponds to birefringence phase-matching (BPM) [1,2]. However, BPM conditions are strongly limited by the refractive indices of the material and they usually forbid the exploitation of the highest coefficient of the second-order electric susceptibility tensor. To overcome this limitation, quasi-phase matching (QPM) is a powerful alternative. It is based on a periodical modulation of the sign of the second-order optical nonlinear coefficient of anisotropic or isotropic non-centrosymmetric crystals [3,4]. We propose here the development and the experimental validation of a new scheme of QPM that allows us to enlarge the spectral range of phase-matched generation and to get access to giant spectral acceptances. For that purpose, we studied Second-Harmonic Generation (SHG) in the ferroelectric periodically-poled Rubidium-doped $KTiOPO_4$ crystal (PPRKTP) [5].

The key parameter of QPM is the periodicity Λ of the spatial modulation of the second-order nonlinearity along the direction of propagation of three interacting waves such as their wavelengths fulfil: $1/\lambda_3 - 1/\lambda_1 - 1/\lambda_2 = 0$. Actually, the goal is to compensate the spatial phase-mismatch $\overrightarrow{\Delta k} = \overrightarrow{k_3} - \overrightarrow{k_1} - \overrightarrow{k_2}$, with $\left|\overrightarrow{k_p}\right| = \frac{2\pi}{\lambda_p} n_p$ where n_p is the refractive index at the wavelength λ_p (p = 1, 2, 3). Then the QPM relation writes [3]:

$$\overrightarrow{\Delta k} = m\overrightarrow{k_\Lambda} \qquad (1)$$

where $\overrightarrow{k_\Lambda}$, with $\left|\overrightarrow{k_\Lambda}\right| = \frac{2\pi}{\Lambda}$, is the grating vector oriented along the propagation direction, and m is the order of the Fourier series. Usually, m is chosen as a positive integer ($m \geqslant 1$), as it is the case for instance while targeting the largest nonlinear coefficient $\chi^{(2)}_{33}$. It is shown in Fig. 1 (left) in the optimal case, i.e. for the lowest QPM positive order m = 1. This is the classical scheme of QPM that we called QPM-A. However, it is also possible to consider propagation directions where $m \leqslant -1$. This configuration has been previously theoretically considered, but without any phenomenological interpretation or experimental verification [6]. We called here this new scheme QPM-B. As for the case of positive orders, the lowest QPM-B order (namely m = -1) shown in Fig. 1 (right) leads to the best efficiency compared to higher

QPM-B orders (namely m < -1), which requires the shortest needed QPM periodicity.
New efficient directions for parametric frequency conversion are expected while using QPM-B since the corresponding phase-matching relation is different from that of QPM-A.

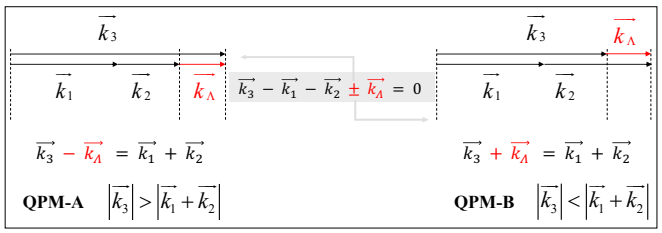

Fig. 1. Schemes of collinear first-order Quasi-Phase-Matching (QPM). $\vec{k}_\Lambda$, where $|\vec{k}_\Lambda| = \frac{2\pi}{\Lambda}$ is the grating vector along the propagation direction and Λ is the periodicity of the spatial modulation of the sign of the second-order non-linearity along the propagation direction; $\vec{k}_1, \vec{k}_2$ and $\vec{k}_3$ are the wave vectors of the interacting waves: positive first-order QPM-A (left), negative first-order QPM-B (right).

Note that from the configuration of polarization, there is no difference between QPM-A (m = 1) and QPM-B (m = -1) because in both cases, there are $2^3 = 8$ possible configurations of refractive index. Actually, since PPRKTP is a birefringent crystal, there are 2 possible refractive indices, *i.e.* n_p^+ and n_p^- with $n_p^+ > n_p^-$, for each of the three interacting waves ($p = 1,2,3$) in the direction of propagation that is considered. These combinations are the following: : type I $\{n_3^-, n_1^+, n_2^+\}$, type II $\{n_3^-, n_1^-, n_2^+\}$, type III $\{n_3^-, n_1^+, n_2^-\}$, type IV $\{n_3^-, n_1^-, n_2^-\}$, type V $\{n_3^+, n_1^+, n_2^+\}$, type VI $\{n_3^+, n_1^-, n_2^+\}$, type VII $\{n_3^+, n_1^+, n_2^-\}$ and type VIII $\{n_3^+, n_1^-, n_2^-\}$ [6]. Note that Type V corresponds to the standard QPM configuration while considering PPRKTP and isotypes, the one that allows the highest nonlinear coefficient d_{33} to be excited.

There is also no difference between the two cases (m = 1, m = -1) in the initial phases φ_1, φ_2 and φ_3 of the three interacting waves when Eq. (1) is fulfilled, i.e. for a perfect QPM. Actually, in this case the phases are locked in such a way that the relation $\varphi_3 - \varphi_1 - \varphi_2 = \pm \pi/2$, as in the case of BPM [1].

From the corpuscular point of view, the QPM condition $\overrightarrow{\Delta k}_{QPM} = \overrightarrow{\Delta k} - m\overrightarrow{k_\Lambda} = \overrightarrow{k_3} - \overrightarrow{k_1} - \overrightarrow{k_2} - m\overrightarrow{k_\Lambda} = \vec{0}$, can be seen as a m+3 particle-interaction, with three photons from the three interacting waves and m quasi-particles with individual momentum $\overrightarrow{k_\Lambda}$ but no energy, which depicts the momentum transfer possibly supported by the nonlinear lattice. In this sense, QPM cases with positive m orders depict interactions where the nonlinear grating transfers momentum, *i.e.* m times the quantized value $\overrightarrow{k_\Lambda}$, to the generated photon at $\overrightarrow{k_3}$. For the lowest positive order (m = 1) three particles with $\overrightarrow{k_1}, \overrightarrow{k_2}$ and $\overrightarrow{k_\Lambda}$ are consumed to produce a new particle associated to $\overrightarrow{k_3} = \overrightarrow{k_1} + \overrightarrow{k_2} + \overrightarrow{k_\Lambda}$. This is somehow similar what occurs while considering the four-particle interaction that corresponds to Third Harmonic Generation (THG) governed by the third-order optical nonlinearity. For the lowest negative order (m = -1) two particles with $\overrightarrow{k_1}$ and $\overrightarrow{k_2}$ are consumed to produce a new pair of particles, one being the new photon associated to $\overrightarrow{k_3}$ and the other one being a momentum quantum $\overrightarrow{k_\Lambda}$ transferred to the grating, while verifying $\overrightarrow{k_3} + \overrightarrow{k_\Lambda} = \overrightarrow{k_1} + \overrightarrow{k_2}$ [7]. This is similar to another four-particle interaction corresponding to four-wave mixing (FWM). Another instructive analogy deals with light diffraction by a periodic acoustic wave under the Bragg condition in a thick acoustic grating configuration. In such a quasi-elastic diffraction condition, it is well established that both positive and negative first-order Bragg interactions exist and are associated either to the annihilation or creation of an acoustic phonon, respectively [8].

From the thermodynamics point of view, efficient QPM can occur whatever the sign of the evolution of the phase mismatch between the nonlinear polarization and the generated optical field. As a consequence, although we generally deal with optical materials with normal spectral dispersion (namely $\partial n/\partial\lambda < 0$), the generalized QPM approach with positive or negative orders would also apply to materials with an anomalous spectral dispersion (namely $\partial n/\partial\lambda > 0$). Because QPM most generally deals with materials with normal dispersion, situations where $\overrightarrow{\Delta k} = m\,\overrightarrow{k_\Lambda} \neq \vec{0}$ with $m > 0$ mostly occur, while $\overrightarrow{\Delta k} = \vec{0}$ is reached for BPM situations. In this sense, the existence of BPM solutions is expected to be a necessary condition to access QPM-B solutions. As a consequence, the QPM-B condition can be fulfilled only for types that can exhibit BPM, so that only Types I, II and III are likely to be addressed by QPM-B schemes in materials with normal dispersion of their refractive indices.

We used an experiment of Angular-Quasi-Phase-Matching (AQPM) for the validation of QPM-B. AQPM is a generalization of QPM since the interacting waves are allowed to propagate at any angle with respect to the grating vector $\overrightarrow{k_\Lambda}$, giving then access to new spectral ranges and giant spectral acceptances [9-11]. Then, it can be applied to QPM-A as well as QPM-B, leading to the so-called AQPM-A and AQPM-B used in the following. In these cases, the grating periodicity Λ has to be replaced by an effective periodicity defined along the collinear propagation direction as follows:

$$\Lambda_{eff}(\theta, \phi) = \Lambda/|\sin(\theta)\cos(\phi)| \qquad (2)$$

Equation (2) gives the grating period as seen in the direction of propagation that is considered, with the angles of spherical coordinates θ and ϕ in the dielectric frame (X,Y,Z) [5]. $\Lambda_{eff}(\theta, \phi)$ ranges from a minimal value corresponding to a propagation in the x-axis that is orthogonal to the domains plane, *i.e.* $\Lambda_{eff}(\theta = 90°, \phi = 0°) = \Lambda$, to a maximal value when the propagation occurs in the YZ plane that is parallel to the domains plane, *i.e.* $\Lambda_{eff}(\theta, \phi = 90°) \to \infty$. The last situation corresponds to BPM, so that the QPM solutions converge for continuity reasons to the BPM solutions, while approaching the YZ plane. It is important to notice that the wave vectors of the three interacting waves remain collinear during an AQPM-B, as it is the case for AQPM-A [9].

The measurements were carried out in the PPRKTP biaxial crystal with a grating period of $\Lambda = 38.52$ µm, as it has been done in our previous study to determine the conditions of AQPM-A for SHG ($1/\lambda_\omega + 1/\lambda_\omega \to 1/\lambda_{2\omega}$). The corresponding curves are plotted in Fig. 2 [10]. We considered the same fundamental wavelength, *i.e.* $\lambda_\omega = 2.15$ µm for the present study of AQPM-B. At this wavelength, using Eqs. (1) and (2) and the Sellmeier equations of reference [12], AQPM-B is expected to be possible for both type I and type II (the

latter being equivalent to type III in the case of SHG), as shown in Fig. 2. We experimentally focused on type II because the conversion efficiency of Type I AQPM-B is more than one order of magnitude smaller than that of type II, as it is also the case for BPM. Moreover, the tuning curve of Type II AQPM-B does not cross any other SHG BPM or AQPM curve as shown in Fig. 2, leading to an unambiguous identification of these newly proposed solutions.

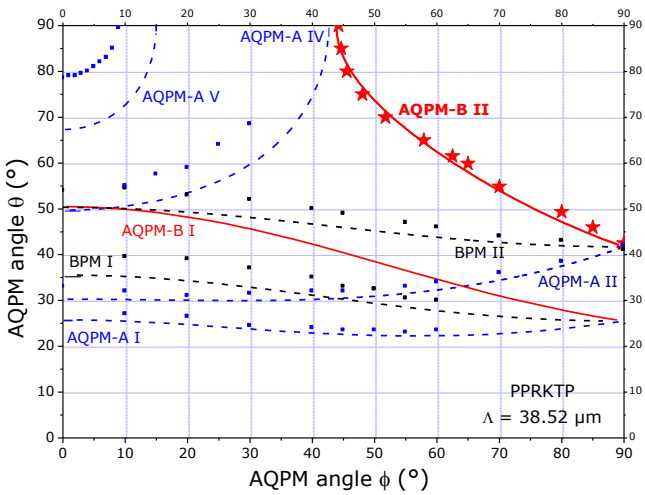

Fig. 2. Second-Harmonic Generation for a fundamental wavelength of λ_ω = 2.15 µm in a PPRKTP crystal with a grating period Λ = 38.52 µm and shaped as a sphere: calculated Types I and II BPM angles (black dashed lines), calculated Types I, II, IV and V AQPM-A angles (blue dashed lines), Types I and II AQPM-B angles (red continuous lines for the calculations and red stars for the present measurements). Black and blue squares are the experimental results obtained in a previous work [11]. θ and ϕ are the angles of spherical coordinates in the dielectric frame (X,Y,Z): ϕ = 0° corresponds to the XZ plane, ϕ = 90° to the YZ plane, and θ = 90° to the XY plane.

The PPRKTP crystal with a grating period of Λ = 38.52 µm was cut as a sphere in order to be able to access any direction of propagation, with the goal of being able to determine all AQPM-B directions. The sphere, with a diameter of 4.76 mm, was oriented by the Laue method, mounted on a goniometric head, and placed at the center of a motorized Kappa circle allowing the sphere to rotate on itself, as shown in Fig. 3 [10]. A homemade interfacing program enables the correspondence between the angles of the spherical coordinates (θ, ϕ) and the Kappa circle angles (κ, Φ_κ, Ω_κ) depicted in Fig. 3. In order to get the whole type II AQPM-B curve, the sphere was successively oriented along the x-axis and the z-axis for orientations verifying 42° ⩽ θ ⩽ 65° and 65° ⩽ θ ⩽ 90°, respectively. A pump beam with a fundamental wavelength of 2.15 µm was emitted by a nanosecond BBO Optical Parametric Oscillator. It was carefully focused at the center of the PPRKTP sphere, which enabled a collimated propagation of the incident beam along the diameter of the crystal sphere [9]. The polarization of the incident beam was controlled with a half-wave plate. The SHG phase-matching angles corresponded to the orientations leading to a maximal value of the associated conversion efficiency that was detected using an amplified Si Hamamatsu C2719 photodiode. A NIRquest 512 Ocean Optics spectrometer, with an accuracy of ±3 nm, was used to control and confirm the same phase-matching wavelength for each of the 12 experimental points shown in Fig. 2.

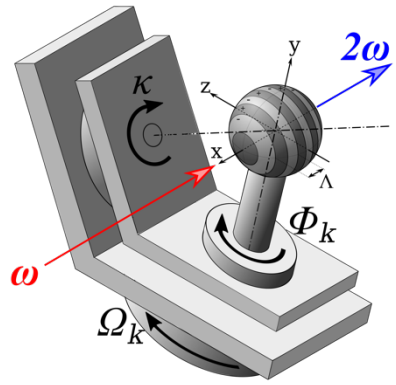

Fig. 3. Schematic diagram of the experiment of Second-Harmonic Generation ($\omega + \omega \rightarrow 2\omega$) used for the determination of the angular distribution of QPM-B. (X,Y,Z) is the dielectric frame of the PPRKTP sphere with a grating period Λ. The sphere is placed at the centre of a Kappa circle whose rotation angles are (κ, Φ_κ, Ω_κ).

The agreement between the measured and calculated phase-matching curves is excellent, hence providing a clear demonstration of type II AQPM-B in PPRKTP, and thus the proof-of-concept for negative order QPM. Based on the existence of these new AQPM schemes, we investigated numerically the associated benefit in terms of spectral tunability and associated spectral acceptances. Calculations of SHG solutions were performed in the XY plane, as this plane is associated with high effective nonlinear coefficients for distinct AQPM types, such as types II and V.

As shown in Fig. 4(a), Type II BPM led to solutions for λ_ω spanning from 0.994 µm to 1.079 µm, and from 3.180 µm to 3.308 µm. Type II AQPM-A showed different solutions in distinct spectral ranges, with λ_ω spanning from 0.952 µm to 0.994 µm, and from 3.308 µm to 4.377 µm. Type II AQPM-B completed the spectral range of the SHG interaction in the XY plane, with λ_ω spanning from 0.994 µm to 3.308 µm. Type V AQPM-A covers the spectral range from 2.057 µm to 3.099 µm. Non-critical spectral conditions are evidenced at λ_ω = 1.567 µm for type II AQPM-B and at λ_ω = 2.503 µm for Type V AQPM-A, when ϕ = 25.53° and 23.22°, respectively. The associated spectral acceptances were determined from the full width at 0.405 of the sinc^2 interference function. It comes: L.δλ = 76 nm.cm at λ_ω = 1.567 µm for Type II AQPM-B, and 161 nm.cm at λ_ω = 2.503 µm for Type V AQPM-A, as shown in Fig. 4(b). Thus, it appears that the proposed AQPM-B scheme opens new potentialities, especially as it provides giant acceptances in the telecom spectral range for PPRKTP.

To ensure that the calculated situations considered in Fig. 4 are practically relevant, it is pertinent to consider the figure of merit (FOM), which is classically defined as:

$$\text{FOM}\ (\theta,\phi) = \frac{d_{\text{eff}}^2(\theta,\phi)}{n_{2\omega}(\theta,\phi)\cdot n_{1,\omega}(\theta,\phi)\cdot n_{2,\omega}(\theta,\phi)} \qquad (3)$$

The quantity $d_{\text{eff}}(\theta,\phi)$ is the effective coefficient, and $n_{i,\omega}(\theta,\phi)$ with i = 1 or 2, and $n_{2\omega}(\theta,\phi)$ are respectively the refractive indices of the fundamental and second-harmonic waves in the direction of propagation that is considered.

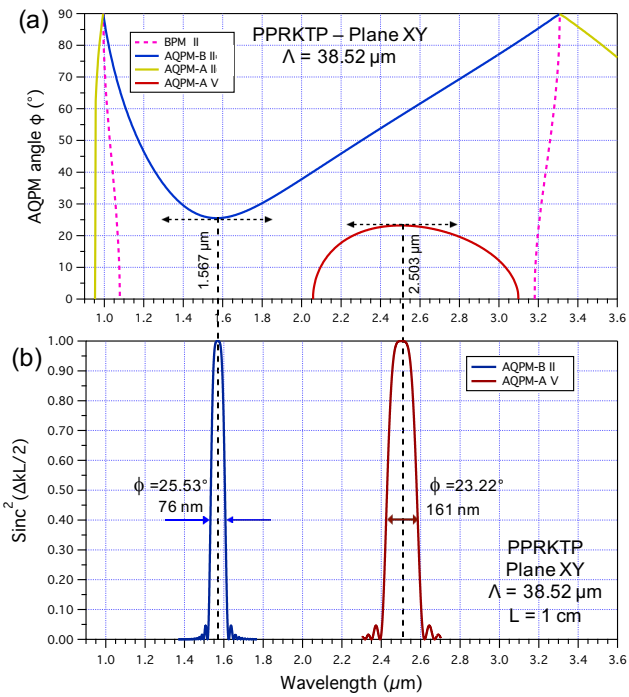

Fig. 4. (a) Spherical AQPM angle ϕ versus fundamental wavelength λ_ω for SHG solutions in the XY dielectric plane of the PPRKTP crystal with the poling period $\Lambda = 38.52$ µm: type II BPM (dashed pink line); type II AQPM-A and type II AQPM-B (yellow and blue lines, respectively); and type V AQPM-A (red line). (b) Spectral dependence of the $\text{sinc}^2(\Delta kL/2)$ interference function for a crystal length L = 1 cm under the undepleted pump approximation (UPA) and at the non-critical wavelengths for type II AQPM-B SHG (λ_ω = 1.567 µm, fixed solution angle at ϕ = 25.53°, blue line), and for type V AQPM-A (λ_ω = 2.503 µm, fixed solution angle at ϕ = 23.22°, red line).

In Table 1 are given the FOM for the two non-critical situations depicted in Fig. 4 where the wavelength acceptances are the broadest, *i.e.* Type V AQPM-A at (ϕ = 23.22°, λ_ω = 2.502 µm) and Type II AQPM-B at (ϕ = 25.53°, λ_ω = 1.567 µm). The values of the refractive indices and nonlinear coefficients d_{15} and d_{24} that are used come from reference [12]. The walk-off angle that is negligible in the XY plane of PPRKTP has been omitted.

Table 1. Figure of merit, FOM (θ= 90°, ϕ), values in the XY plane for type II AQPM-B and type V AQPM-A at non-critical spectral conditions.

AQPM Type (plane XY)	λ_ω (µm)	ϕ (°)	Effective Coefficients (d_{eff})	FOM
II-B	1,567	25,53	$\frac{2}{\pi}(d_{15}sin^2\phi + d_{24}cos^2\phi)$	0,36
V-A	2,503	23,22	$\frac{2}{\pi}(d_{33})$	5,16

Note that the effective nonlinear coefficient is defined by the same expression for both the positive and negative first-order QPM conditions given a type and the associated polarization configuration. As a consequence, the effective nonlinear coefficient contains a Fourier factor of 2/π since we consider the first-order modulation of the sign of the nonlinearity, as in the case of AQPM-A. However, the effective coefficient shows different values, as it is estimated along distinct propagation directions, respectively corresponding to the AQPM-A and AQPM-B solutions of Eq. (1). Even if the FOM of Type V AQPM-A in the XY plane is 14 times higher than that of Type II AQPM-B, the FOM value for Type II AQPM-B is not negligible and it shows real practical potential as this interaction occurs in the telecom C-band close to 1.55 µm.

In conclusion, we performed a comprehensive interpretation and experimental validation of a generalized description of the QPM interaction by incorporating negative QPM orders, in addition to the well-known positive ones. We have labelled QPM with negative orders as the QPM-B cases, contrarily to the QPM-A cases with positive QPM orders. We have demonstrated the existence of such QPM-B situations in the case of type II SHG with a fundamental beam at 2.15 µm in a PPRKTP crystal exhibiting a period Λ = 38.52 µm perpendicularly to the ferroelectric domains. We have highlighted that AQPM-B gives access to extended spectral ranges and non-critical spectral tolerances. A giant spectral tolerance of 76 nm.cm at λ_ω = 1.567 µm was determined for type II AQPM-B in the XY plane, which interestingly lies in the telecom spectral range. The associated figure of merit was estimated to be 0.36. The generalized QPM description enlarges the palette of QPM interactions and widens the interaction of nonlinear interactions in periodically-poled media. Knowing the diversity of BPM cones of solutions and the even larger one for the AQPM-A case [2,13], the newly demonstrated negative QPM solutions keep on enlarging the possibilities of favourable configurations for cascaded nonlinear parametric frequency conversion interactions, while considering simultaneous phase-matching and/or positive/negative quasi-phase matching conditions. Finally, this approach naturally extends to other periodically poled uniaxial crystals such as the periodically-poled $LiNbO_3$ (PPLN).

Funding. Centre National de la Recherche Scientifique (CNRS) International Project of Scientific Cooperation France – Sweden (PICS no. 7739).

Disclosures. The authors declare no conflicts of interest.

References

1. J. A. Armstrong, N. Bloembergen, J. Ducuing, and P. S. Pershan, Phys. Rev. **127**, 1918 (1962).
2. J. P. Fève, B. Boulanger, and G. Marnier, Opt. Commun. **99**, 284 (1993).
3. M. M. Fejer, G. A. Magel, D. H. Jundt, and R. L. Byer, IEEE J. Quantum Electron. **28**, 2631 (1992).
4. A. Arie, N. Voloch, Laser & Photon. Rev. **4** (3), 355 (2010).
5. A. Zukauskas, N. Thilmann, V. Pasiskevicius, F. Laurell, and C. Canalias, Opt. Mater. Express **1**, 201 (2011).
6. V. Pasiskevicius, S. J. Holmgren, S. Wang, and F. Laurell, Opt. Lett. **27**(18), 1628 (2002).
7. J.P. Fève, B. Boulanger and J. Douady, Phys. Rev. A **66**, 063817 (2002).
8. B. E. A Saleh and M. C. Teich, Wiley series in pure and applied Optics, Fundamentals of Photonics (second Edition, 2007).
9. Y. Petit, B. Boulanger, P. Segonds, and T. Taira, Phys. Rev. **A 76**, 063817 (2007).
10. P. Brand, B. Boulanger, P. Segonds, Y. Petit, C. Félix, B. Ménaert, T. Taira, and H. Ishizuki, Opt. Lett. **34**, 2578 (2009).
11. D. Lu, A. Peña, P. Segonds, J. Debray, S. Joly, A. Zukauskas, F. Laurell, V. Pasiskevicius, H. Yu, H. Zhang, J. Wang, C. Canalias, B. Boulanger, Opt. Lett. **43**, 4276 (2018).
12. K. Kato and E. Takaoka, Appl. Opt. **41**, 5040 (2002).
13. Y. Petit, P. Brand, P. Segonds, B. Boulanger, Optical Materials **32**, 1501–1507 (2010).

Full references

1. J. A. Armstrong, N. Bloembergen, J. Ducuing, and P. S. Pershan, "Interactions between light waves in a nonlinear dielectrc", Phys. Rev. **127**, 1918-1939 (1962). DOI: 10.1103/PhysRev.127.1918

2. J. P. Fève, B. Boulanger, and G. Marnier, "Calculation and classification of the direction loci for collinear type-I, type-II and tipe-III phase-matching of 3-wave nonlinear-optical parametric interactions in uniaxial and biaxial acentric crystals" Opt. Commun. **99**, 284-302 (1993). DOI: 10.1016/0030-4018(93)90092-J

3. M. M. Fejer, G. A. Magel, D. H. Jundt, and R. L. Byer, "Quasi-phase-matched 2nd harmonic-generation-tuning and tolerances", IEEE J. Quantum Electron. **28**, 2631-2654 (1992). DOI: 10.1109/3.161322

4. A. Arie, N. Voloch, "Periodic, quasi-periodic, and random quadratic nonlinear photonic crystals", Laser & Photonics Reviews **4** (3), 355-373 (2010).

5. A. Zukauskas, N. Thilmann, V. Pasiskevicius, F. Laurell, and C. Canalias, "5 mm thick periodically poled Rb-doped KTP for high energy optical parametric frequency conversion", Opt. Mater. Express **1**, 201-206 (2011). DOI: 10.1364/OME.1.000201

6. V. Pasiskevicius, S. J. Holmgren, S. Wang, and F. Laurell, "Simultaneous second-harmonic generation with two orthogonal polarization states in periodically poled KTP", Optics Letters **27**(18), 1628-1630 (2002).

7. J.P. Fève, B. Boulanger and J. Douady, "Specific properties of cubic optical parametric interactions compared to quadratic interactions", Phys. Rev. A **66**, 063817 (2002). DOI: 10.1103/PhysRevA.66.063817

8. B. E. A Saleh and M. C. Teich, Wiley series in pure and applied Optics, Fundamentals of Photonics (second Edition, 2007).

9. Y. Petit, B. Boulanger, P. Segonds, and T. Taira, "Angular quasi-phase-matching", Phys. Rev. **A 76**, 063817 (2007). DOI: 10.1103/PhysRevA.76.063817

10. P. Brand, B. Boulanger, P. Segonds, Y. Petit, C. Félix, B. Ménaert, T. Taira, and H. Ishizuki, "Angular quasi-phase-matching experiments and determination of accurate Sellmeier equations for 5%MgO:PPLN" Opt. Lett. **34**, 2578-2580 (2009). DOI: 10.1364/OL.34.002578

11. D. Lu, A. Peña, P. Segonds, J. Debray, S. Joly, A. Zukauskas, F. Laurell, V. Pasiskevicius, H. Yu, H. Zhang, J. Wang, C. Canalias, B. Boulanger, "Validation of the angular quasi-phase-matching theory for the biaxial optical class using PPRKTP", Opt. Lett. **43(17)**, 4276-4279 (2018). DOI: 10.1364/OL.43.004276

12. K. Kato and E. Takaoka, "Sellmeier and thermos-optic dispersion formular for KTP", Appl. Opt. **41**, 5040-5044 (2002). DOI: 10.1364/AO.41.005040

13. Y. Petit, P. Brand, P. Segonds, B. Boulanger, "Classification of angular quasi-phase-matching loci in periodically poled uniaxial crystals", Optical Materials **32(11)**, 1501–1507 (2010). DOI: 10.1016/j.optmat.2010.06.011